Studies on Thermal Degradation of Cellulose and Cellulose Phosphoramides

BALJINDER KAUR, I. S. GUR, and HARI L. BHATNAGAR,
Department of Chemistry, Kurukshetra University, Kurukshetra 132119, India

Synopsis

Reaction of cellulose with hexamethylphosphoric acid triamide has been investigated under various physical conditions. Dimethylamine hydrochloride was found to be an efficient catalyst for the system. The thermal degradation of cellulose and its phosphoramide products in air was studied by DTA, TG, and DTG techniques from ambient temperature to 500°C. The data were processed for the various thermodynamic parameters following the methods of Freeman and Carroll, of Broido, and of Dave and Chopra. The energies of activation, E_a, for the degradation for various cellulose phosphoramide samples were found to be in the range of 92–136 kJ mol^{-1}. These values were found to decrease with increase in the degree of substitution. A mechanism for the thermal degradation of cellulose phosphoramide has been proposed. The IR spectra of char residues of cellulose phosphoramide gave an indication of the formation of compounds containing C=O and P=O groups.

INTRODUCTION

Cellulose, when exposed to ignition source, will decompose and produce among other things gaseous products which ignite, propagate the flame, and further decompose the cellulose until only ash remains. The primary role of flame retardant is to change the decomposition process in such a way that the amount of flammable gases produced is minimized, and correspondingly the amount of char formed is increased.[1] Hendrix et al.[2] studied the action of phosphorus-containing compounds on cotton and suggested that dephosphorylation followed by an acid-catalyzed dehydration and thermal decomposition of the treated cotton occurred on burning. Tesoro and co-workers[3,4] have described the nitrogen–phosphorus interdependence as being synergistic. Hendrix et al.[2] suggested that phosphorus–nitrogen synergistic effect may be due to the formation of a more effective catalyst for cellulose degradation by the interaction of the phosphorus and nitrogen compounds, or the nitrogen may react directly with the products of cellulose decomposition.

This presentation describes the preparation of cellulose derivatives of hexamethylphosphoric acid triamide (HPAT) and their kinetics of thermal degradation in air atmosphere from ambient temperature to 500°C using dynamic TG, DTG, and DTA techniques. The values of different kinetic parameters have been obtained by employing different techniques.[5–7] Infrared spectra of samples, heated to significant temperatures of pyrolysis, have been analyzed in an effort to obtain more information concerning the flame-retardant mechanism of cellulose derivatives.

Journal of Applied Polymer Science, Vol. 31, 667–683 (1986)
 CCC 0021-8995/86/020667-17$04.00

EXPERIMENTAL

The following samples of cellulose and its derivatives were selected for the present work: sample (i) cellulose (from Dassel, West Germany) dried *in vacuo* at 60°C; samples (ii)–(v) obtained by treating cellulose (2 g) with HPAT (6 g) in dimethylformamide at 80, 100, 120 ± 0.5°C for 24 h and 150 ± 0.5°C for 12 h, respectively, in the presence of 1% dimethylamine hydrochloride (DMA·HCl) as catalyst; and sample (vi) obtained by the above reaction at 150 ± 0.5°C for 12 h in the absence of catalyst. The products obtained were filtered, rinsed with excess $CHCl_3$ to remove unreacted HPAT, washed thoroughly with distilled water, and dried over P_2O_5 *in vacuo*. Phosphorus was estimated by the colorimetric method.[8] Nitrogen was determined by the Kjeldahl method.

Thermogravimetry, Derivative Thermogravimetry and Differential Thermal Analysis

The TG, DTG, and DTA thermograms were obtained using an MOM derivatograph (Paulik, Paulik and Erdey, Budapest, Hungary). The amount of samples (i)–(v) taken for these studies was 100 mg in each case and for sample (vi) it was 90 mg. The TG, DTG, and DTA curves were run under a dynamic air atmosphere at a constant heating rate of 10°C/min.

Infrared Studies

For IR studies, KBr discs containing 2% charred products of sample (ii) were prepared and analyzed using Beckman Spectrophotometer IR-20 (United States). The charred samples were prepared in a DTA cell. Heating was stopped at the desired temperature, and the residues after cooling were quickly transferred to sample containers.

THEORETICAL ASPECTS

Determination of Kinetic Parameters

The kinetic parameters for the decomposition of samples (i)–(vi) were determined using the methods described by Freeman and Carroll,[5] Broido,[6] and Dave and Chopra.[7] The equations involved in the various methods are given below:

(A) Freeman and Carroll Method[5] (from TG Curve).

$$\frac{\Delta \log R_T}{\Delta \log W} = n - \frac{E_a}{2.303R} \cdot \frac{\Delta(1/T)}{\Delta \log W} \tag{1}$$

Rate of decomposition[9]

$$-\frac{dW}{dT} = R_T = \frac{Z}{\mathrm{RH}} \exp\left(-\frac{E_a}{\mathrm{RT}}\right) \cdot W^n$$

where W is weight fraction of the sample undergoing degradation with temperature at time t, RH is the rate of heating (°C/min), and Z is the frequency factor.

(B) Broido Method[6] (from TG Curve).

$$\ln\left(\ln\frac{1}{y}\right) = -\frac{E_a}{R}\cdot\frac{1}{T} + \ln\left(\frac{R}{E_a}\cdot\frac{Z}{\mathrm{RH}}\cdot T_m^2\right) \tag{2}$$

where y is the fraction of number of initial molecules not yet decomposed and T_m is the temperature of maximum reaction rate.

(C) Dave and Chopra Method[7] (from DTG Curve).

$$k_1 = \frac{(A/M_0)^{n-1}(-dx/dt)}{(A-a)^n} \tag{3}$$

where k_1 is rate constant, A is the total area (mg) under the DTG curve, a is the area (mg) for the reaction up to time t, dx/dt is the height of the curve (mg/min) at time t, M_0 is initial mole fraction of the reactant, and n is the order of reaction. The Arrhenius equation was utilized for evaluating the energies of activation.

RESULTS AND DISCUSSION

Reaction of HPAT with cellulose is expected to yield a phosphite ester[10] represented by formula:

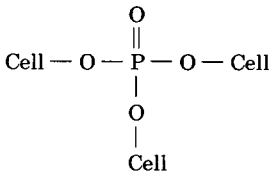

This product is expected if the reaction goes to completion. If the reaction does not go to completion, then compound II or III is expected:

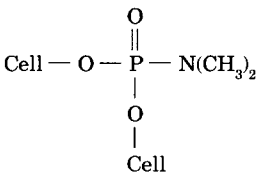

(II)

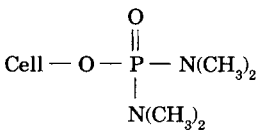

(III)

Some of the dimethyl amine groups may be replaced by hydroxyl groups during washings, leading to compound

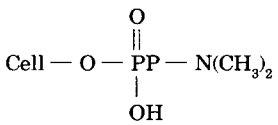

(IV)

Dimethylamine hydrochloride has been seen to be effective catalyst[11] for the alcoholysis of phosphorous acid amides. The use of 1% catalyst caused considerable increase in the percentage of phosphorus and nitrogen. Also, phosphorus and nitrogen contents increased with the increase in the temperature of the reaction as can be seen in Table I.

Although thermal decomposition of cellulose is a complex process, the reaction products may be classified into three distinct categories; a series of gaseous products, primarily water and carbon dioxide; a solid carbonaceous char; and rather ill-defined tar which decomposes further with production of various flammable gases. It is shown by various workers[12,13] that the main constituent of this tar is 1,6-anhydroglucopyranose (levoglucosan), and it is this decomposition to levoglucosan which plays an important role in the flammability of celluloses.

The DTA thermograms of cellulose and samples (ii)–(vi) were recorded in air. The peak temperatures for the various endotherms and the exotherms are given in Table I. An endotherm below 120°C in all these compounds is due to the evaporation of sorbed moisture. For samples (ii)–(vi), an endotherm is observed in the range of 215–235°C, depending upon the percent of P and N. This endotherm may be accounted for dephosphorylation and simultaneous decomposition of the samples by the catalytic effect of the released acids. The next peak, an exotherm in the temperature range 320–350°C, is due to oxidative decomposition of the products. The last exotherm in the range 372–468°C is due to oxidation of char.

Dynamic TG and DTG for samples (i)–(vi) are shown in Figures 1–6. First DTG maxima in samples (ii), (iii), (iv), and (vi) are at 246, 243, 232, and 235°C, respectively (Table II). This is due to dephosphorylation reaction. The next maxima in these samples at 310, 300, 274, and 279°C (Table III) may be accounted for decomposition reaction. In sample (v), there is only one maximum at 238°C, indicating that, in this case, dephosphorylation and decomposition reactions are taking place simultaneously. The char yields (wt %) were obtained from the TG curves and given in Table IV. From DTA and DTG curves, it is evident that there is (a) lowering in decomposition temperature, (b) decrease in temperature at which maximum weight loss occurs, and (c) increase in char in cellulose derivatives with increasing percentage of P and N. This shows that hexamethylphosphoric acid triamide is an effective flame retardant as the main role[1] of flame retardant is to lower the decomposition temperature so that minimum volatile products are formed and correspondingly higher amount of charred residue is left.

In TGA curves, the initial rapid but small weight loss is due to loss of sorbed moisture and was neglected. The kinetic parameters for various stages of pyrolysis were determined using the Broido[6] method. The Dave–Chopra[7] method was applied to first and second stage of the pyrolysis, whereas the Freeman–Carroll[5] method was applied to second stage only. It has been observed that each method has its own advantages in a particular range of pyrolysis.

From the slopes of TG curves in Figures 1–6, plots of $\Delta \log R_T/\Delta \log W$ vs. $\Delta (1/T)/\Delta \log W$ [eq. (1)] were made and are shown in Figure 7. The activation energies E_a and the order of reaction, n, were determined from

TABLE I
Peak Temperatures in the DTA Thermograms for Cellulose and Cellulose Derivatives in Air

Sample no.	Sample	P (%)	N (%)	Peak temperature (°C)			Nature of the peak
				Initiation	Maxima	Termination	
(i)	Cellulose	—	—	260	314	325	(Endo (large)
				325	350	405	Exo (large)
				405	468	520	Exo (large)
(ii)	Cellulose treated with HPAT at 80°C	4.10	1.78	158	235	310	Endo (large)
				310	350	360	Exo (large)
	for 24 h			360	372	466	Exo (small)
(iii)	Cellulose treated with HPAT at 100°C	5.58	2.48	154	233	301	Endo (large)
				301	348	378	Exo (large)
	for 24 h			378	392	478	Exo (small)
(iv)	Cellulose treated with HPAT at 120°C	7.06	3.12	143	227	275	Endo (large)
				275	330	392	Exo (large)
	for 24 h			392	404	472	Exo (small)
(v)	Cellulose treated with HPAT at 150°C	10.82	4.20	125	215	251	Endo (large)
				251	320	372	Exo (large)
	for 12 h			372	380	435	Exo (small)
(vi)	Cellulose treated with HPAT at 150°C	6.30	2.71	146	235	284	Endo (large)
				284	334	376	Exo (large)
	for 12 h without catalyst			376	388	445	Exo (small)

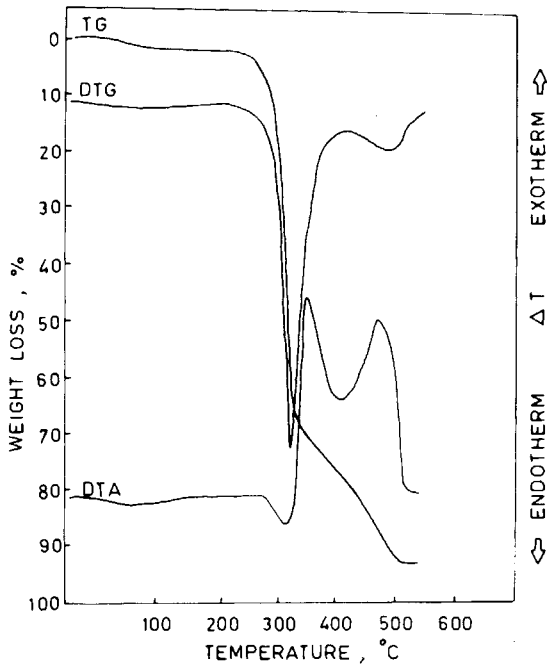

Fig. 1. Thermal analysis of cellulose in air (——) and in nitrogen (- - -).

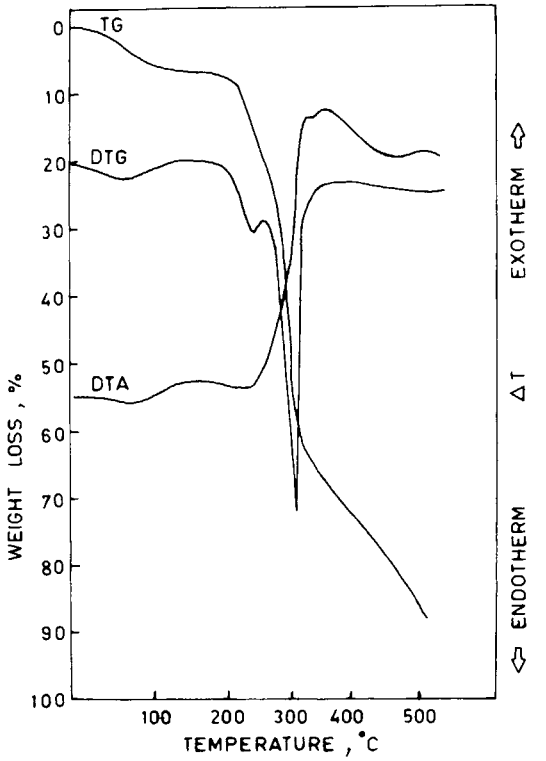

Fig. 2. Thermal analysis of cellulose phosphate I in air (——) and in nitrogen (- - -).

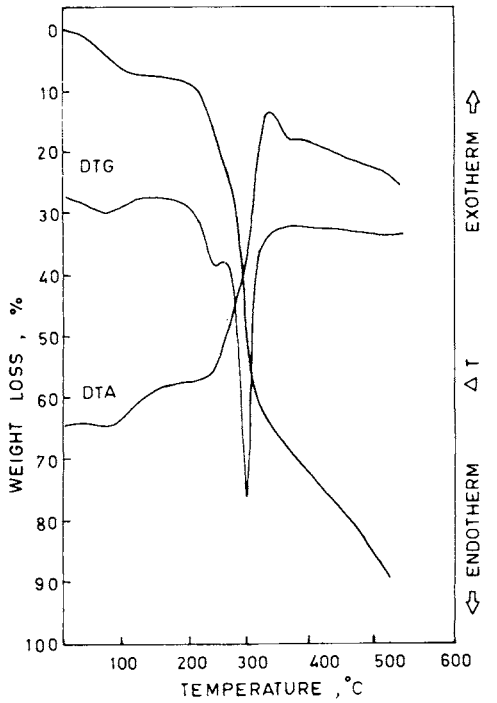

Fig. 3. Thermal analysis of cellulose diethylphosphate in air (——) and in nitrogen (- - -).

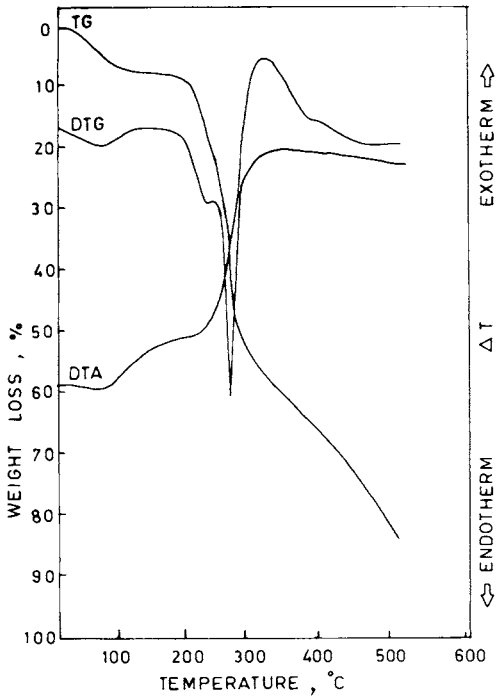

Fig. 4. Thermal analysis of cellulose diphenylphosphate in air (——) and in nitrogen (- - -).

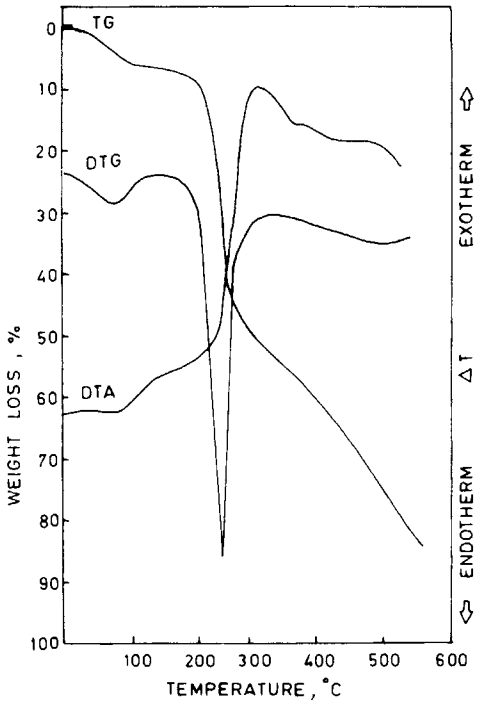

Fig. 5. Thermal analysis of cellulose phosphate II in air (——) and in nitrogen (- - -).

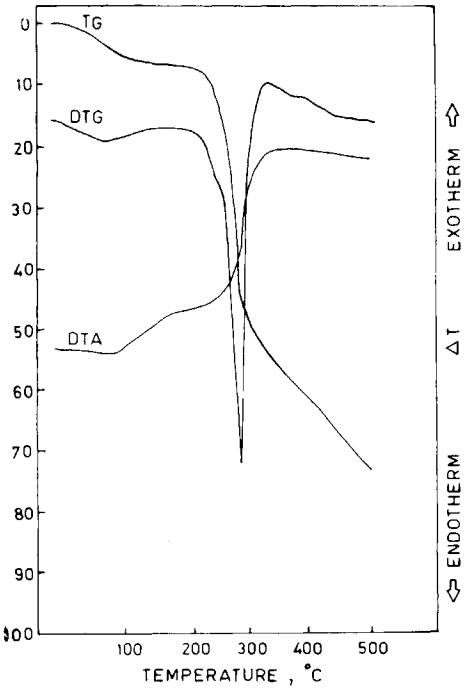

Fig. 6. Thermal analysis of cellobiose phosphate I in air (——) and in nitrogen (- - -).

TABLE II
Activation Energies and Frequency Factors for First Stage of Pyrolysis of Cellulose and Cellulose Derivatives in Air

Sample no.	DTG maxima (°C)	Temperature range (°C)	E_a (kJ mol^{-1}) Broido method	E_a (kJ mol^{-1}) Dave–Chopra method	Z (s^{-1}) Broido method	Z (s^{-1}) Dave–Chopra method
(i)	—	240–285	172.1	180.9	1.36×10^{13}	3.36×10^{13}
(ii)	246	200–260	129.4	11.6	6.54×10^{11}	1.95×10^{8}
(iii)	243	200–260	117.7	111.8	3.83×10^{10}	2.36×10^{8}
(iv)	232	190–240	124.4	130.1	4.26×10^{11}	4.84×10^{10}
(v)	—	175–210	89.8	91.3	9.77×10^{7}	3.19×10^{6}
(vi)	235	200–245	127.9	118.8	3.83×10^{11}	1.09×10^{9}

[1a] Compounds referred to as sample nos. (i)–(vi) are same as in Table I.

the Broido method, plots of $\ln(\ln 1/y)$ vs. $1/T$ [eq. (2)] for the various stages of pyrolysis were drawn and are given in Figures 8–10. The activation energies E_a and the frequency factors Z determined from the slopes and the intercepts of these plots respectively are given in Tables II–IV. Using the Dave–Chopra method, the values of k_1 obtained from eq. (3) were plotted against $\frac{1}{T}$ (Figs. 11–12). The values of energy of activation, E_a, and the frequency factor Z were calculated and are given in Tables II and III. These parameters were evaluated using the least squares method in all the cases.

For the first stage of pyrolysis, mainly dephosphorylation and dehydration, the values of the energies of activation (Table II) lie in the range of 89–130 kJ mol^{-1}, which are low as compared to pure cellulose (172 kJ mol^{-1}). The energies of activation of samples (ii)–(vi) for second stage of pyrolysis are in the range of 92–136 kJ mol^{-1}. The values of the activation energy for the third stage of pyrolysis are in the range of 92–110 kJ mol^{-1}.

From Tables II–IV, it is clear that values of the energy of activation depend upon the method employed and also, energies of activation of treated samples decrease with increasing percentage of P and N, showing thereby that the charring temperature of treated samples is in decreasing order.

Mechanism of Pyrolysis

The most generally accepted mechanism for pyrolysis of cellulose phosphoramide consists of first the generation of phosphoric acid amide.[14] This acid then alters the pyrolytic decomposition of cellulose in such a way that primary decomposition products are changed from levoglucosan and other flammable products of cellulose to carbonaceous char.[15]

Phosphoric acid amide is generated according to the well-known thermal degradation reaction of the alkyl phosphorus esters to an olefin and the corresponding acid:

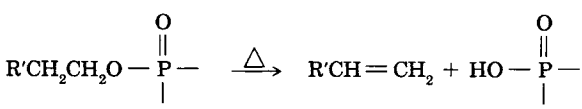

TABLE III
Activation Energies and Frequency Factors Using Different Methods for Second (Decomposition) Stage of Pyrolysis of Cellulose and Its Derivatives in Air

Sample no.[a]	DTG maxima (°C)	Temperature range (°C)	E_a (kJ mol^{-1})			Z(s^{-1})			n
			Broido method	Freeman–Carroll method	Dave–Chopra method	Broido method	Freeman–Carroll method	Dave–Chopra method	
(i)	321	285–335	238.4	212.8	242.4	2.18×10^{19}	1.82×10^{18}	1.62×10^{19}	1.05
(ii)	310	260–370	133.1	123.2	136.8	2.31×10^{11}	3.16×10^{10}	1.14×10^{10}	1.007
(iii)	300	260–370	129.4	117.8	137.1	1.51×10^{11}	1.32×10^{10}	1.69×10^{10}	1.001
(iv)	274	240–340	119.3	115.0	126.5	7.29×10^{10}	2.95×10^{10}	1.32×10^{10}	0.92
(v)	238	210–380	99.4	92.1	106.7	1.78×10^{9}	5.19×10^{8}	6.90×10^{8}	0.97
(vi)	279	245–360	136.4	135.5	129.8	2.23×10^{12}	2.16×10^{12}	1.89×10^{10}	0.97

[a] Compounds referred to as sample nos. (i)–(vi) are same as in Table I.

TABLE IV
Activation Energies and Frequency Factors for the Third Stage of Pyrolysis of Cellulose and Its Derivatives in Air, using Broido Method

Sample no.[a]	Temperature range (°C)	E_a (kJ mol^{-1})	Z (s^{-1})	Char yield at 770 K (wt %)
(i)	335–500	187.1	1.03×10^{11}	7.8
(ii)	370–500	110.9	8.90×10^{6}	14.5
(iii)	370–500	103.6	2.75×10^{6}	15.5
(iv)	340–500	92.6	5.31×10^{5}	18.0
(v)	380–500	110.1	6.94×10^{6}	24.0
(vi)	360–500	100.1	1.63×10^{6}	18.5

[a] Compounds referred to as sample nos. (i)–(vi) are same as in Table I.

Based on this reaction, thermal degradaton of cellulose phosphoramide leading to char formation, can be depicted as in Scheme I. The mechanism has been discussed in detail elsewhere.[16]

Phosphoric acid amide, generated on heating, can polymerize to form polyphosphoramide, which is more effective catalyst in dehydration reaction. It initially phosphorylates cellulose and phosphorylated cellulose then breaks down to give water, phosphoric acid amide and dehydrated char. This can be depicted as in Scheme II.

In addition to the above-mentioned dehydration mechanism via esterification with polyphosphoramide, dehydration can also occur by a single acid-catalyzed elimination of water. The acid-catalyzed dehydration of cel-

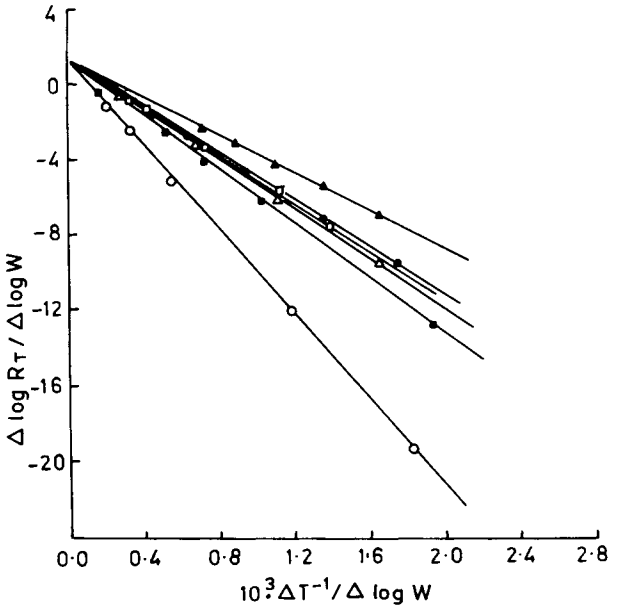

Fig. 7. Plots of ln(ln $1/y$) vs. $10^3 \times T^{-1}/K^{-1}$ using the Broido equation for cellulose (●), cellulose diethylphosphate (■), cellulose diphenylphosphate (○), and cellulose phosphate II (△) in air (a) and in nitrogen (b) for first stage of pyrolysis.

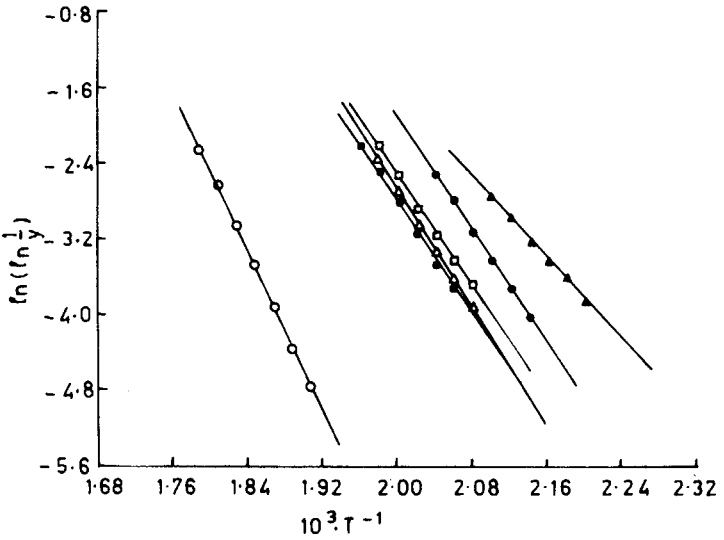

Fig. 8. Plots of ln(ln $1/y$) vs. $10^3 \times T^{-1}/K^{-1}$ using the Broido equation for cellulose (●), cellulose phosphate I (▲), cellulose diethylphosphate (■), cellulose diphenylphosphate (○), cellulose phosphate II (△), and cellobiose phosphate I (□) in air (a) and in nitrogen (b) for second stage of pyrolysis.

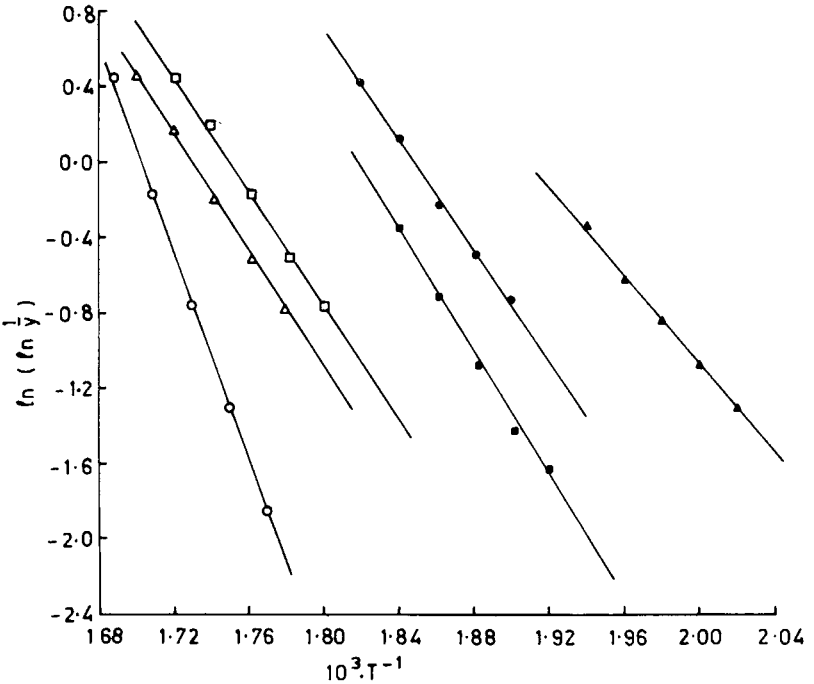

Fig. 9. Plots of ln(ln $1/y$) vs. $10^3 \times T^{-1}/K^{-1}$ using the Broido equation for cellulose (●), cellulose phosphate I (▲), cellulose diethylphosphate (■), cellulose diphenylphosphate (○), cellulose phosphate II (△), and cellobiose phosphate I (□) in air (a) and in nitrogen (b) for third stage of pyrolysis.

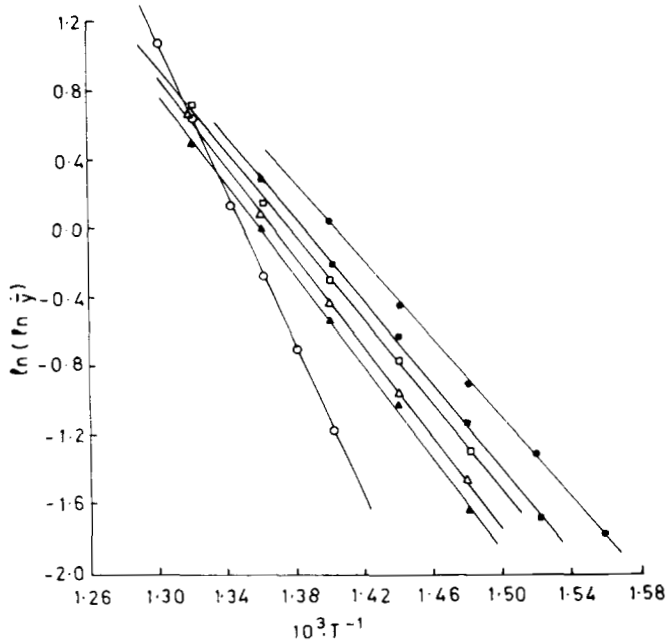

Fig. 10. Plots of ln(ln 1/y) vs. $10^3 \times T^{-1}/K^{-1}$ using the Broido equation for cellulose (●), cellulose phosphate I (▲), cellulose diethylphosphate (■), cellulose diphenylphosphate (○), cellulose phosphate II (△), and cellobiose phosphate I (□) in air (a) and in nitrogen (b) for fourth stage of pyrolysis.

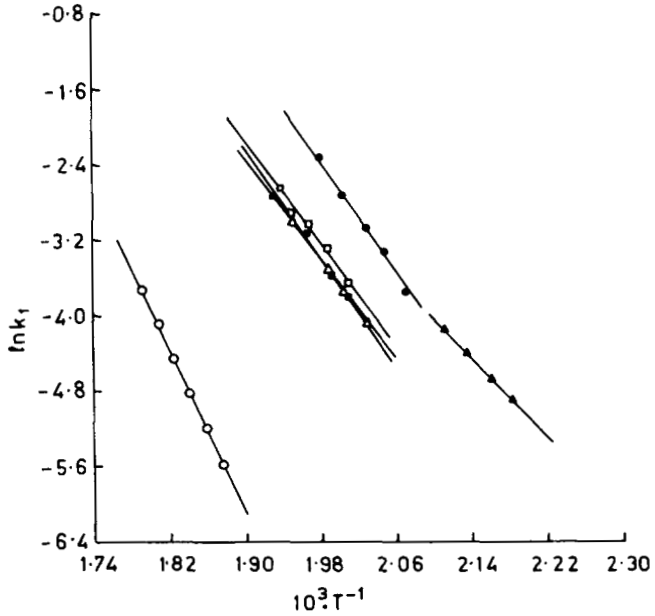

Fig. 11. Plots of (Δ log R_T/Δ log W) vs. ($10^3 \times \Delta\ T^{-1}/\Delta$ log $W)/K^{-1}$ using Freeman and Carroll equation for cellulose (●), cellulose phosphate I (▲), cellulose diethylphosphate (■), cellulose diphenylphosphate (○), cellulose phosphate II (△), and cellobiose phosphate I (□) in air (a) and in nitrogen (b) for second stage of pyrolysis.

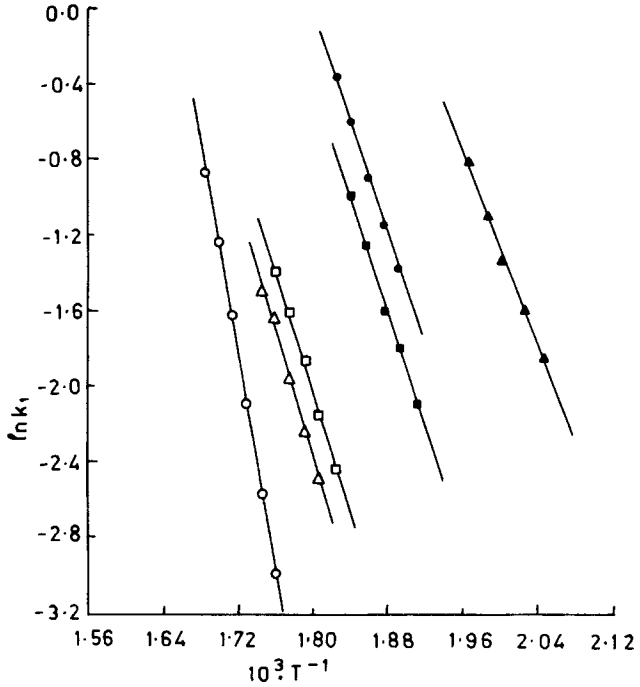

Fig. 12. Mass spectrum of cellobiose phosphate I.

lulose at primary hydroxyl groups results in the formation of an exocyclic methylene, whereas at secondary hydroxyl groups, it results in endocyclic double bond. This is shown in Scheme III.

The fact that all phosphorus compounds, which are capable of decomposing to acid fragments are effective fire retardants for cellulose, supports this mechanism. Acid-catalyzed dehydration of cellulose is further supported by the fact that esters of strong mineral acids, such as sulfuric acid, are also effective fire retardants for cellulose, although they are not as efficient as phosphorus acids.

The infrared spectra of residual products of cellulose phosphoramide also

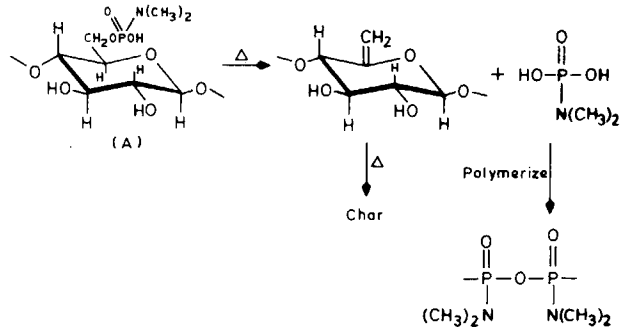

Scheme I. Thermal Degradation of Cellulose Phosphates

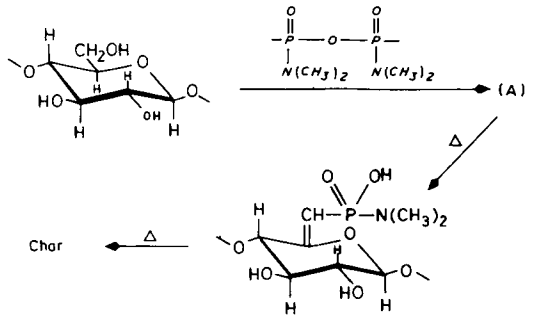

Scheme II. Thermal Degradation of Cellulose Phosphates

confirm these observations. Sample (v) was subjected to pyrolysis in air and the IR spectra of the chars formed at different temperatures were recorded (Fig. 13). The spectrum for the char obtained at 200°C showed no change in absorption bands, while that for char at 225°C showed evidence for dehydration by decrease in the intensities of absorption bands due to hydroxyl stretching (3300–3400 cm^{-1}) and bending (1320, 1380 cm^{-1}). Also, the bands at 2900 [—C—H (pyranose ring)str], 1160 (antisym. bridge C—O—C str), 1125 and both 1060 and 1035 cm^{-1} (skeletal vibrations involving C—O str), etc., showed decrease, indicating degradation of cellulose phosphoramide along with dehydration. The vibration band due to P=O stretching shifted from 1200 to 1250 cm^{-1}. This may be accounted for dephosphorylation and then catalytic effect of phosphoramide group. Also at this temperature, there was indication of skeletal rearrangement as evidenced by appearance

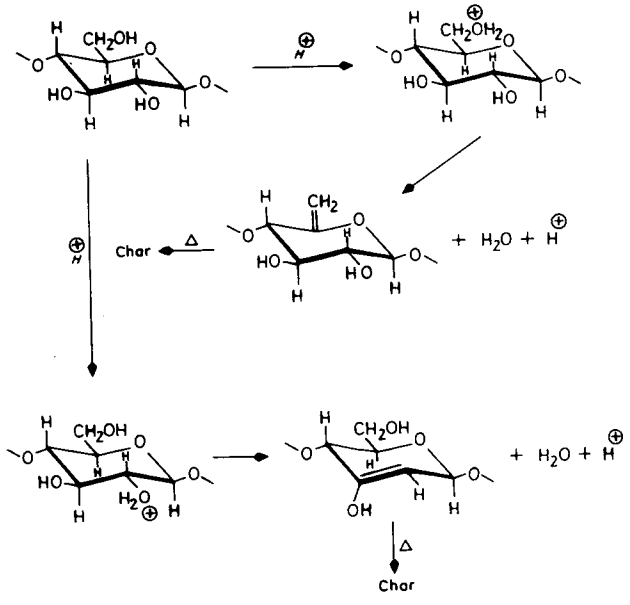

Scheme-III

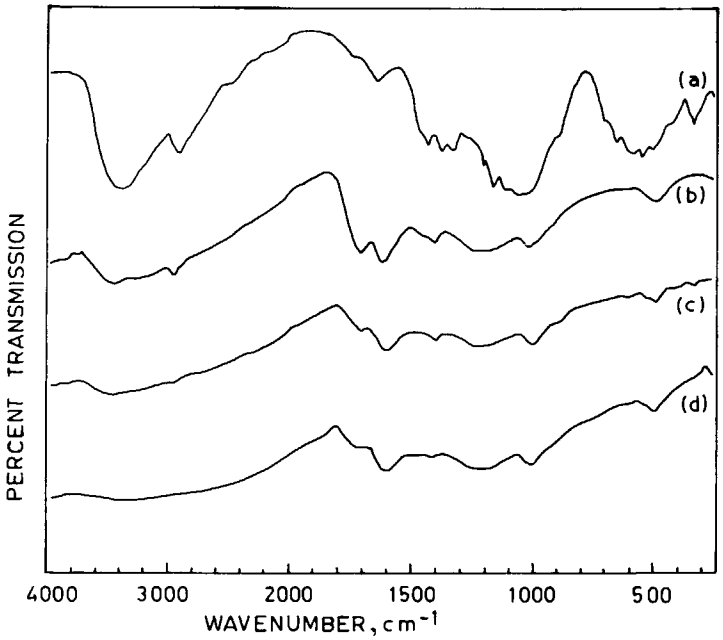

Fig. 13. IR spectra of (a) cellulose phosphate I and (b–e) chars of cellulose phosphate I at different temperatures (b) 125°C, (c) 150°C, (d) 200°C, and (e) 250°C.

of new bands at 1720 (C=O str) and 1000 cm^{-1} (=C—H bending) and shifting of bands from 1440 (—CH_2 bending) and 1640 cm^{-1} (conjugated C=C) to 1400 and 1600 cm^{-1}, respectively. At 350°C, all normal bands due to cellulose phosphoramide disappeared completely, and intense bands at 1720 (C=O), 1600 (C=C), 1400 (—CH_2), 1250 (P=O), and 1000 cm^{-1} (=C—H) remained, suggesting the formation of compounds containing C=O and P=O groups.

One of the authors (B. K.) is grateful to the Council of Scientific and Industrial Research, New Delhi for providing a research fellowship.

References

1. R. M. Perkins, G. L. Drake, Jr., and W. A. Reeves, *J. Appl. Polym. Sci.*, **10**, 1041 (1966).
2. J. E. Hendrix, J. E. Bostic, Jr., E. S. Olson, and R. H. Barker, *J. Appl. Polym. Sci.*, **14**, 1701 (1970).
3. G. C. Tesoro, *Textilveredlung*, **2**, 435 (1967).
4. G. C. Tesoro, S. B. Sello, and J. J. Willard, *Text. Res. J.*, **38**, 245 (1968).
5. E. S. Freeman and B. Carrol, *J. Phys. Chem.*, **62**, 394 (1958).
6. A. Broido, *J. Polym. Sci., Part A-2*, **7**, 1761 (1969).
7. N. G. Dave and S. K. Chopra, *Z. Physik Chem.*, **48**, 257 (1966).
8. W. A. Pons, Jr. and J. D. Guthrie, *Ind. Eng. Chem.*, **18**, 184 (1946).
9. L. Reich and S. S. Stivala, *Elements of Polymer Degradation*, McGraw-Hill, New York, 1971, p. 102.
10. A. B. Pepperman, Jr. and L. H. Chance, *J. Appl. Polym. Sci.*, **16**, 1833 (1972).
11. E. E. Nifant'ev, N. L. Ivanova, and N. K. Bliznyuk, *Zh. Obshch. Khim.*, **36**, 765 (1966).

12. J. E, Hendrix and R. H. Barker, *Clemson Univ. Rev. Ind. Management Text. Sci.*, **8**, 63 (1969).
13. F. Shafizadeh, *Adv. Carbohydr. Chem.*, **23**, 419 (1968).
14. J. E, Hendrix and G. L. Drake, Jr., *J. Appl. Polym. Sci.*, **16**, 257 (1972).
15. J. W. Lyons, *J. Fire Flammability*, **1**, 302 (1970).
16. Rajesh K. Jain, Krishan Lal, and Hari L. Bhatnagar, *J. Appl. Polym. Sci.* (1984), to appear.

Received December 11, 1984
Accepted June 20, 1985